MICROSTRUCTURAL SIMULATION OF HOT FORMING PROCESSES

C. Sommitsch, V. Wieser
Boehler Edelstahl GmbH & Co KG, P.O.Box 96, A-8605 Kapfenberg, Austria

Abstract
Semi-empirical and physically based models for the simulation of hot forming processes have been developed. For nickel-base superalloys, Avrami type equations embedded in a commercial finite element program can estimate the grain structure development during and after the deformation. The physically based model consists of several modules for the calculation of the thermodynamic equilibrium, the diffusion, the precipitation kinetics and the grain structure development, which are coupled with the finite element code. In the field of industrial hot forming processes, such models are used to optimise the deformation procedure and to predict the final microstructure.

Keywords: Hot forming, Rolling, Forging, Nickel-base Superalloys, Microstructure, Simulation, Recrystallisation, Precipitation, Modelling

Introduction

Steel producers are currently striving to model their process lines in order to optimise the manufacturing process and to achieve the desired microstructure and mechanical properties. There are commercial finite element programs for the calculation of process parameters in the fields of melting, solidification, re-melting, hot deformation and heat treatment. However, considerable emphasis is being placed on developing numerical procedures to describe the evolution of microstructure and to couple them with finite element code.
The present paper is concerned with the calculation of the microstructure of nickel-base alloys during rolling and forging, both by semi-empirical and physically based models. An Avrami type model [1] for the prediction of the grain structure is embedded in the programme code of DEFORM^{TM}. An example of this kind of model is presented for an open die forging process (cogging) of the alloy 718.
On the other hand, physically based simulation of hot deformation processes is much more complex, depending on the scale of modelling and on whether or not physical processes and their interactions are considered. The present model [2] contains several modules for the calculation of the thermodynamic equilibrium, the diffusion in a multi-component, multi-phase system, the precipitation kinetics with a classical nucleation and growth theory [3] and a statistical dislocation density model [4] which considers recrystallisation and grain growth and determines the actual flow stress. To get reasonable simulation results the boundary conditions (friction, heat transmission,…) and their dependencies have to be known. For the model validation a comprehensive experimental program on a Gleeble 3800 has been conducted [4]. Both a rolling step within the multi-line rolling mill and a heat treatment of an ingot was modelled for the alloy 80A as an example of physically based modelling.

Semi-empirical model

In metals with low stacking fault energies such as austenitic steels and nickel-base alloys, recrystallisation is the dominant softening mechanism during hot deformation. Reaching sufficiently high local strains (dislocation density gradients) and temperatures leads to the nucleation and growth of new grains [5]. The concurrent deformation stimulates an ongoing nucleation if a critical strain is reached. Thus the microstructure contains grains having different

sizes and straines. If the strain rate equals the recrystallisation rate, a stationary flow stress is reached. The maximum stress for a given temperature T and strain rate $\dot{\varepsilon}$ can be described [6] by

$$\sinh(\alpha \sigma_{max}) = A Z^m \quad (1),$$

where Z denotes the Zener-Hollomon parameter and α, A and m are constants:

$$Z = \dot{\varepsilon} \exp\left(\frac{Q_{def}}{RT}\right) \quad (2)$$

and Q_{def} is the activation energy for deformation.
The critical strain for the start of dynamic recrystallisation (DRX) is proportional to the strain at σ_{max} and depends on the initial grain size d_0

$$\varepsilon_{cr} = k_{cr}\, \varepsilon_p = A_\varepsilon\, d_o^{l}\, Z^{m_\varepsilon} \quad (3)$$

where k_{cr}, A_ε and m_ε are constants. The recrystallised fraction can be described using an Avrami type equation

$$X = 1 - \exp\left[\ln(1-x)\left(\frac{t}{t_x}\right)^k\right] \quad (4).$$

Here the exponent k is a constant and t_x is the time for recrystallisation [7] of the volume fraction x

$$t_x = B d_0^r\, \varepsilon^{-s}\, Z^{-b} \exp\left(\frac{Q_{rx}}{RT}\right) = B d_0^r\, \dot{\varepsilon}^{-b} \exp\left(\frac{Q_{rx} - b Q_{def}}{RT}\right) \quad (5),$$

B, r, s and b are constants and Q_{rx} denotes the apparent activation energy for recrystallisation. The recrystallised grain size d is given by

$$d = J Z^{-y} \quad (6),$$

where J and y depend on the composition.

In the case of post-dynamic static recrystallisation (PDSR) or static recrystallisation (SRX), the local temperature changes with time, which can be considered by a temperature compensated time W_x [7] where for constant temperature

$$W_x = t_x \exp\left(-\frac{Q_{rx}}{RT}\right) = B d_0^r\, \varepsilon^{-s}\, Z^{-b} \exp\left(\frac{Q_{def}}{RT}\right) \quad (7)$$

and for changing temperature

$$W_i = \exp\left(-\frac{Q_m}{RT_i}\right) t_i \quad (8).$$

The recrystallised fraction is given by

$$X_i = 1 - \exp\left[\ln(1-x)\left(\frac{W_i}{W_x}\right)^n\right] \quad (9),$$

where X_i is the recrystallised increment for a time increment at constant temperature and strain rate and n is a constant. The overall apparent temperature sensitivity for postdynamic or static recrystallisation Q is given by

$$Q = Q_m - b Q_{def} \quad (10).$$

The recrystallised grain size can be described by

$$d_m = D d_0^f \varepsilon^g Z^{-h} \quad (11),$$

where D, f, g and h depend on the composition.

In the case of SRX, the final grain size depends sensitively on the initial grain size and the strain, but is not particularly affected by the temperature. This reflects the significant influence of the initial microstructure on the number of nuclei, which is the characteristic that essentially controls the recrystallised grain size. The same principle holds for the grain size after DRX, but since the DRX structure is controlled only by Z, it follows that the DRX grain size, and hence the PDSR grain size, are functions of Z only. Hodgson and Gibbs [8] showed that for a carbon steel the post-dynamic grain size is about 1.5 times the dynamic grain size, and both decrease as Z is increased. Thus, in the case of PDSR, the influences of the initial grain size d_0 and the pre-strain ε in the equations (5, 7, 11) can be neglected. The average grain size after PDSR in the alloy 718 was found to be 1.5-2 ASTM grades larger than after DRX [9]. Reported values for Q for PDSR are 252 kJ/mol for C-Mn steels [10], 123-153 kJ/mol for different C-Mo, C-Ti and C-Nb steels [11], 81 kJ/mol (Q_{rx}=115 kJ/mol) for Waspaloy [12] and 280 kJ/mol (Q_{rx}=389 kJ/mol) for Inconel 718 [14].

Once DRX has started, recrystallisation will always proceed after stopping the deformation, regardless of the strain. Hence for a semi-empirical model it is sufficient to describe PDSR or SRX. The driving force for classical SRX is the minimisation of the deformation energy due to the annihilation of dislocations. The number of nuclei and thus the recrystallised grain size depends on the dislocation energy and the initial grain size. The influence of the deformation rate is negligible. In the case of the onset of DRX the grain size shifts in the direction of stationary grain size (which does not depend on the pre-strain and the initial grain size) and the dislocation density in the direction of a stationary dislocation density. Therefor the grain size and the recrystallised fraction do not depend on the initial grain size or the pre-strain. However the question of where the transition of PDSR to SRX occurs and how far DRX must proceed for the grain size and recrystallised fraction to become independent of strain and initial grain size, remains. Jonas et al. [11] investigated the influence of the pre-strain on PDSR in the region between the strain at maximum stress and the strain at stationary stress for different steel types in the austenitic regime. It appeared that the influence of the pre-strain became small if a significant recrystallised fraction formed. The reason for this is that the density of nuclei for PDSR remains relatively constant in this

case. The dynamically formed nuclei have a growth advantage against nuclei which form after the deformation.
The following example (figures 1,2) describes the open die forging process (cogging) of an ingot of alloy 718. The simulation was carried out using the commercially available finite element package, DEFORM 3D™. The semi-empirical model is written in Fortran code within a program subroutine. The initial temperature was 1130°C and the initial grain size was 100µm. The case modelled was cogging of a 850mm round billet to a 790mm round billet in four forging sequences, each sequence consisting of six impacts.

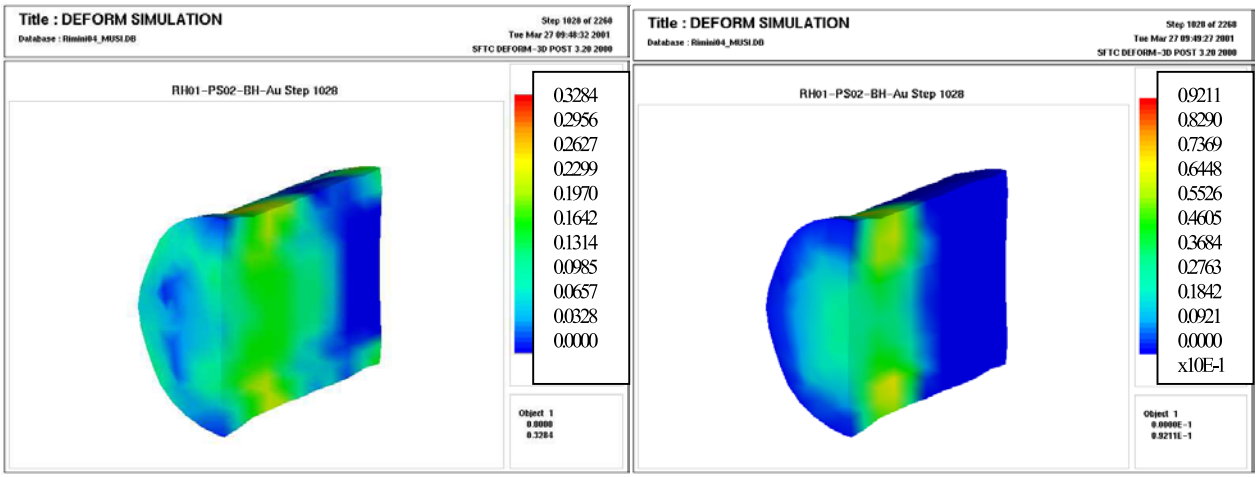

(a) (b)

Fig. 1. Symmetrical half of the ingot during the 2nd forging sequence: (a) effective strain after the 4th impact, (b) mean effective strain rate [1/s] of the 4th impact.

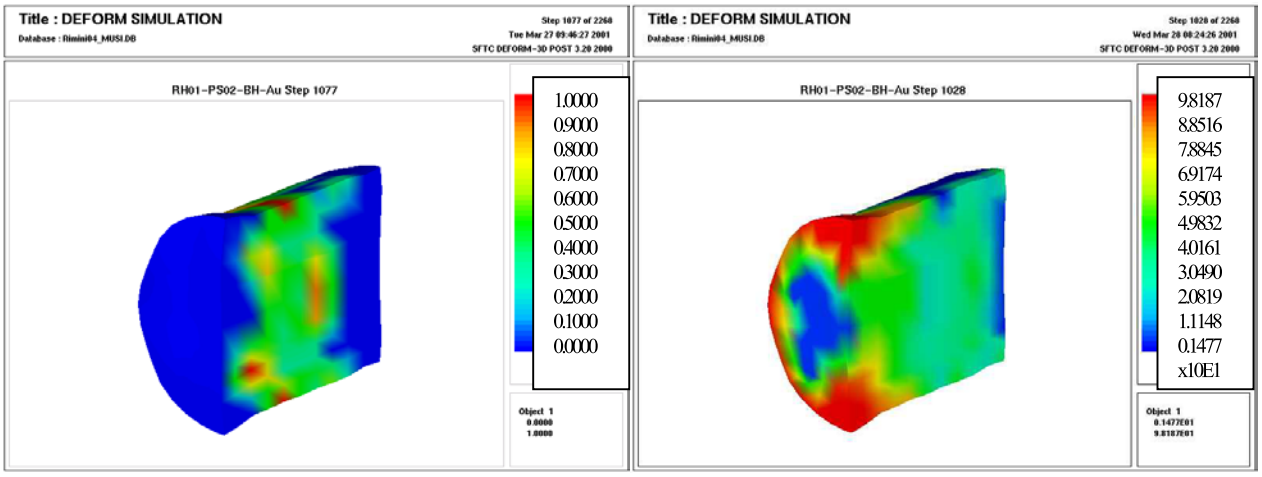

(a) (b)

Fig. 2. Symmetrical half of the ingot during the 2nd forging sequence: (a) postdynamic recrystallised fraction after the 4th impact and 5s delay time, (b) mean grain size [µm] after the 4th impact.

Physical based model

In contrast to the above-mentioned approach, more sophisticated physically based models attempt to describe the kinetic processes and their interactions. A general formulation allows the simulation of microstructural evolution for a whole materials group unlike the semi-empirical models where many fit parameters have to be determined by a comprehensive experimental program for one single alloy. This implies the consideration of precipitation processes and their interaction with moving large angle grain boundaries (recrystallisation, grain growth). Also the flow stress during a current deformation results from the corresponding microstructure. The following model was

developed for the simulation of hot forming processes of nickel-base alloys. Figure (3) shows a flow chart of the numerical model.

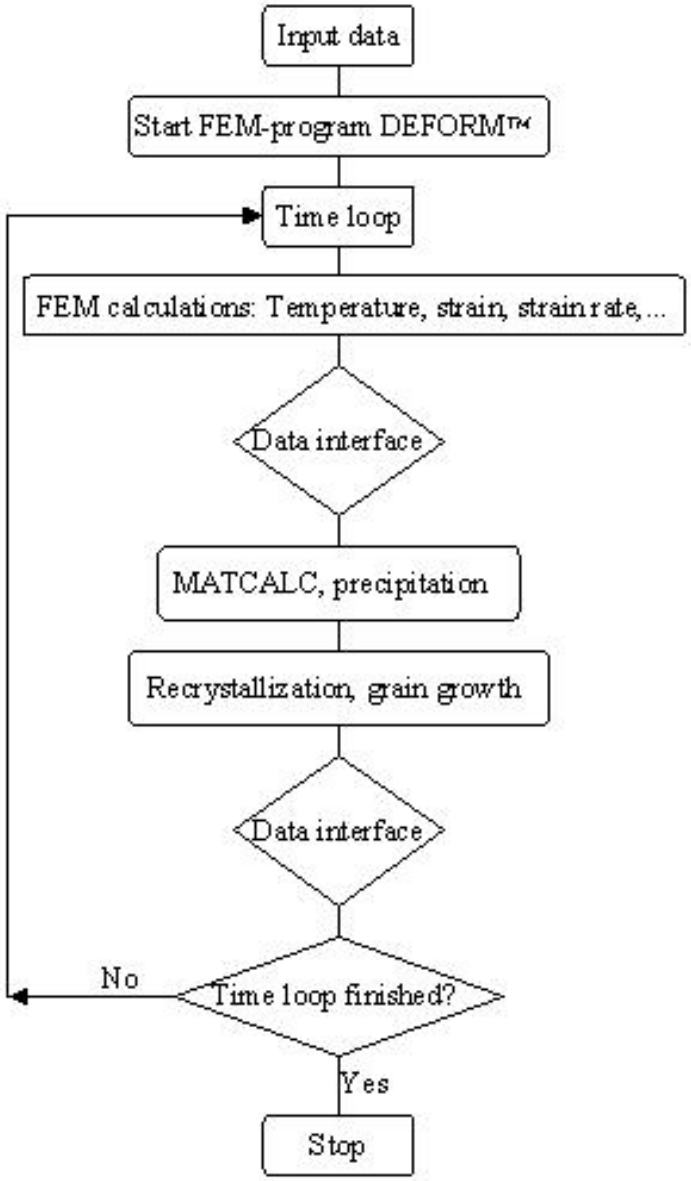

Fig. 3. Flow chart of the numerical model. The data interface handles the management of the node related data, calculated using DEFORM™, and the correlated microstructural data, calculated using the developed program libraries.

Thermodynamic model and multi-component diffusion

The present precipitation model [3] couples an extended Kampmann-Wagner [14] approach for nickel-base alloys with the program MatCalc [15]. The latter is utilised for the evaluation of the driving forces for precipitation, the equilibrium phase compositions and the multi-component diffusion coefficients.

The equilibrium module of the thermokinetic software package MatCalc is based on the minimum total Gibbs free energy principle

$$G_m = \sum_i f^i \cdot G_m^i = Minimum \quad (12),$$

where G_m is the molar Gibbs free energy of the system, G^i_m is the molar Gibbs free energy of a phase i and f^i is the corresponding phase fraction. The thermodynamic formalism describing G^i_m is based on the sublattice model [16] and the thermodynamic parameters are read from available commercial databases, i.e. the nickel-base database [17]. The software structure has recently been described in detail in reference [18].

The chemical diffusion coefficients D that are needed to simulate the growth and coarsening kinetics of precipitates are evaluated using the model of Andersson and Agren [19]. The required mobility data is evaluated using the mobility database of the software package DICTRA [20].

Precipitation model

The precipitation model described here is based on the numerical Kampmann-Wagner model [14], which is derived from classical nucleation and growth theory [21]. Phase separation in solid alloys often occurs as the thermally activated migration of atoms through a phase boundary. Hence, the free energy changes with the free volume energy ΔG_V (chemical formation energy) because of the formation of new phase volume (energy gain), and the free surface energy because of the formation of new interface area (energy loss). In the case of coherent particles, the elastic strain energy ΔG_ε, due to the lattice misfit of the matrix and the particle, must also be considered. The change of the free energy during a nucleation process [22] is therefore

$$\Delta G = -V\left(\Delta G_V - \Delta G_\varepsilon\right) + A\gamma_{\alpha\beta} \quad (13),$$

where V is the volume, A is the surface area of the nucleus and $\gamma_{\alpha\beta}$ is the phase boundary energy (α: matrix, β: precipitated phase). Inserting for the energy contributions in equation (13) and building the extremum for ΔG yields the critical nucleus radius

$$R^* = \frac{2\gamma_{\alpha\beta}}{\Delta G_V - \Delta G_\varepsilon} \quad (14).$$

For heterogeneous nucleation at dislocations and at interfaces, the phase boundary energy can be set to a smaller value due to the fact that the energy barrier for nucleation at inhomogeneities is lower [23]. With these terms, an expression for the nucleation rate J can be derived [24]

$$J(t) = J_s \exp\left(-\frac{\tau}{t}\right) = Z\,\beta^* N_0 \exp\left(-\frac{\Delta G^*}{kT}\right)\exp\left(-\frac{\tau}{t}\right) \quad (15),$$

where J_s is the stationary nucleation rate which is reached after the nuclei (clusters) that formed have a stable size with negligible probability of dissolution and ΔG^* is the critical work of formation. τ indicates the incubation time. N_0 designates the number of potential nucleation sites per unit volume and β^* the rate at which solute atoms from the matrix with mean concentration c join the nucleus. In the present model, both N_0 and β^* depend on the nucleation site and are either related to the lattice parameter (homogeneous nucleation), to the grain size (nucleation at grain boundaries) or to the dislocation density (strain induced nucleation) [25]. The growth rate of an over-critical spherical nucleus is given by

$$\frac{dR}{dt} = \frac{c(t) - c_R}{c_p - c_R}\frac{D}{R} \quad (16),$$

where c_p, $c(t)$ and c_R are the concentrations of the solute in the precipitate, in the matrix and at the interface boundary, respectively. The latter is given in terms of the Gibbs-Thompson equation [26]

$$c_R(R) = c_e \exp\left(\frac{2\gamma_{\alpha\beta}}{R_g T}\frac{V_\beta}{R}\right) \quad (17),$$

where R_g is the universal gas constant, c_e is the equilibrium concentration of the solute in the matrix and V_β is the molar volume of the precipitate phase. The numerical model and the model validation are described elsewhere [3].

Grain structure model

The present model [2, 4] simulates the grain structure development during and after hot deformation of nickel-base alloys. It considers normal grain growth and dynamic, post-dynamic and static recrystallisation and can be used for alloys with low stacking fault energy and thus recrystallisation as the predominant softening process.

Criteria for recrystallisation

During hot forming, the derivative of the dislocation density can be described [27] by the equation

$$\frac{d\rho}{dt} = \frac{\dot{\varepsilon}}{bl} - 2M\tau\rho^2 \quad (18),$$

taking the strain hardening and the recovery of dislocations into account, where $\dot{\varepsilon}$ is the strain rate, b the Burgers vector, l the mean free path of the dislocations, M the mobility of recovery and τ the average energy per unit length of a dislocation.

A critical dislocation density is necessary in order to initiate DRX. The nucleus usually forms at pre-existing grain boundaries in the material, at least at higher strain rates [28]. For an area that has just been recrystallised it is assumed that the dislocation density ρ_0 generated by the preceding strain is reduced to a very low value. The critical dislocation density and the critical size of a nucleus are derived by a nucleation criterion, developed by Roberts and Ahlblom [29], which is based upon the idea that during dynamic recrystallisation the concurrent deformation reduces the stored energy difference (driving force) that effects migration of a high angle boundary.

The velocity of a high angle boundary during recrystallisation is the product of the boundary mobility, m, and the sum of the driving and dragging forces:

$$v = m\,\Delta P = m\left(\tau\,\Delta\rho - P_Z\right)P_S \quad (19),$$

where $\tau\Delta\rho$ is the stored energy difference in the vicinity of the boundary, P_Z the Zener drag [30] and P_S the solute drag for high boundary velocities [31].

Recrystallisation model

In the following it is assumed that nucleation will occur at the grain boundaries (in the grain boundary area F) of the deformed material. F/f_0 is the number of stable nuclei which can be formed where f_0 is the cross sectional area of a critical nucleus. A statistical model where the number of nuclei per volume as a function of time is given by $Z(t)$ can describe the nucleation with time

$$Z(t) = Z_\infty \left(1 - \exp(-\alpha t)\right) \quad (20),$$

where Z_∞ denotes the asymptotic number of nuclei per volume for $t \to \infty$ and α is an exponential variable. It results from preliminary calculations that α has to be proportional to the gradient of the dislocation energy $\tau\rho/d_{gb}$

$$\alpha = \frac{m\tau\rho_\alpha}{d_{gb}} K_\alpha \quad (21),$$

where d_{gb} is the 'thickness' of the grain boundary and K_α is a constant. During recrystallisation, a grain boundary slips over the plane f_p

$$f_p = \pi\left(r_0 + \int_0^t v\,dt\right)^2 - f_0 = \pi\left[\left(\int_0^t v\,dt\right)^2 + 2r_0\int_0^t v\,dt\right] \quad (22),$$

with the assumption that the grain boundary velocity depends on time. This can occur during the recrystallisation process (eq. 20) due to the precipitation of particles, changing temperature and strain rate. The number of annihilated potential nuclei in f_p is ϕ

$$\phi(v,t) = \frac{f_p}{\pi r_0^2} = \left(\int_0^t \frac{v}{r_0}\,dt\right)^2 + 2\int_0^t \frac{v}{r_0}\,dt \quad (23).$$

Because of this annihilation process, the constant factor Z_∞ in eq. (20) becomes time dependent. Hence the recrystallised fraction f is given by

$$f = Z(t)V_m \quad (24),$$

where V_m is the mean volume of the recrystallised grains. Calculating the growth of the recrystallised grains, it must be considered that with time the grains will touch and will form new, immobile boundaries. After this moment only a fraction of the boundary $\Psi(f)$ will move, which is a function of the recrystallised volume fraction, where $\Psi(1)$ has to be zero. The nuclei of the second recrystallisation cycle will form at the contact points of the grains of the first cycle. It seems to be suitable to set the number of contact points in proportion to the fraction of the pinned grain boundary plane $(1-\Psi)$. The total recrystallised volume fraction is assumed to be equal to the fraction of the first cycle because the second recrystallisation front only exists within the recrystallised structure of the first generation. The mean dislocation density of n recrystallisation cycles (also taking into account the unrecrystallised structure with i=0) results from

$$\rho_m = \sum_{i=0}^{n} \rho_{im} f_i \quad (25),$$

where ρ_{im} denotes the mean dislocation density within cycle i. The numerical recrystallisation model and the model validation are described elsewhere [2, 4].

In the following two examples using this model, one for hot rolling of slabs made of the alloy 80A (fig. 4) and the other for a heat treatment of an ingot of alloy 80A (fig. 5) are given.

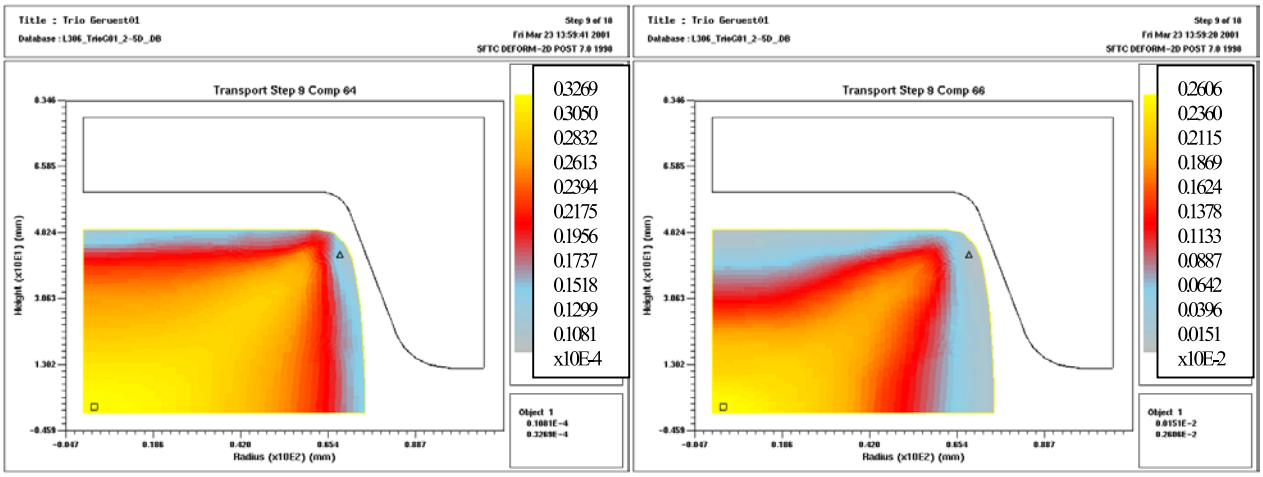

(a) (b)

Fig. 4. Symmetrical quarter of a section of a rolling slab immediately after the rolling pass: (a) velocity [m/s] of the first recrystallisation cycle (eq. 19), (b) fraction of recrystallisation (eq. 24).

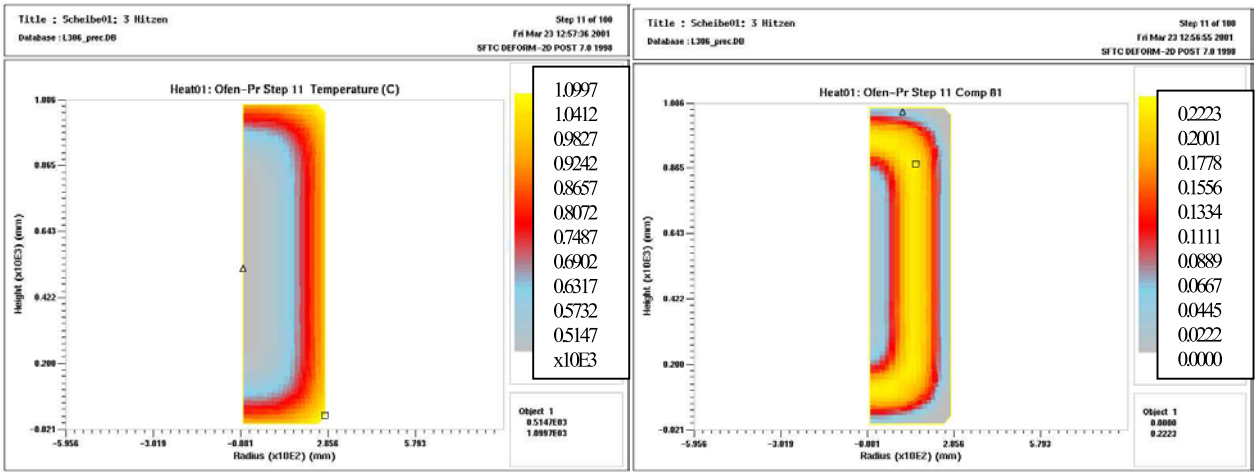

(a) (b)

Fig. 5. Symmetrical half of a section of an ingot during heat treatment: (a) temperature [°C], (b) fraction of γ'-particle.

Conclusions

The models presented here show two attempts of microstructural modelling, a semi-empirical and a physically based approach. Simple Avrami type equations have the advantage that can easily be implemented in the source code of a commercial finite element program and the disadvantage of needing numerous fitting parameters for any single alloy. However, they are only able to give us a glimpse of the ongoing physical processes during a hot forming process. Hence the fundamental physical approach presented above is the more promising model for the future. Due to the long calculation times this type of simulation is only efficient in 2D models at the moment. The module-like structure aids the implementation of different models for the calculation of the microstructure e.g. for the precipitation kinetics or the grain structure development.

References

1) C. SOMMITSCH, V. WIESER, CH. WURM and H. LENGER, *BHMAM* 146 (1), (2001), p.6.
2) C. SOMMITSCH, Ph.D. Thesis, Institute for Materials Science, Welding and Forming, Graz University of Technology, Graz (1999).
3) C. SOMMITSCH and E. KOZESCHNIK, G. WASLE and B. BUCHMAYR, *Proc. THERMEC'2000*, Las Vegas (2000), in print.
4) C. SOMMITSCH and W. MITTER, *Proc. Materials Week 2000*, Munich (2000), http://www.materialsweek.org/proceedings, Werkstoffwoche-Partnerschaft GbRmbH, Munich (2000).
5) T. SAKAI and J.J.JONAS, *Acta metall*. 32, (1984), p.189.
6) C.M. SELLARS and W.J. TEGART, *Acta metall*. 14, (1966), p.1136.
7) C.M. SELLARS and J.A.WHITEMAN, *Metal Sc*. 13, (1979), p.187.
8) P.D. HODGSON and R.K. GIBBS, *ISIJ Int*. 32, (1992), p.1329.
9) P.E. MOSSER, G. LECONTE, J. LERAY, A. LASALMONIE and Y. HONNORAT, *Superalloy 718 – metallurgy and application,* Warrendale (1989), TMS, p.179.
10) A. LAASRAOUI and J.J. JONAS, *ISIJ Int*. 31, (1991), p.95.
11) J.J. JONAS, T. MACCAGNO and S. YUE, *Phase Transformations During the Thermal/Mechanical Processing of Steels,* (1995), The Canadian Institute of Mining, E.B. Hawbolt and S. Yue (Eds.), p.179.
12) G. SHEN, S.L. SEMIATIN and R. SHIVPURI, *Met.Mat.Trans*. 26A, (1995), p.1795.
13) A.J. BRAND, K. KARHAUSEN and R. KOPP, *Mat.Sc.Techn.* 12, (1996), p.963.
14) R. KAMPMANN and R. WAGNER, *Decomposition of Alloys: The Early Stages*, Pergamon Press, Oxford (1984), p.91.
15) E.KOZESCHNIK, Ph.D. Thesis, Institute for Materials Science, Welding and Forming, Graz University of Technology, Graz (1997).
16) M. HILLERT and L.-I. STAFFANSSON, *Acta Chem.Scand.* 24, (1970), p.3618.
17) N. SAUNDERS, *Phil.Trans.* 351A, (1995), p.543.
18) E. KOZESCHNIK and B.BUCHMAYR, *Mathematical Modelling of Weld Phenomena 6*, H. CERJAK, H.K.D.H. BADESHIA (Eds.), Institute of Materials, London (2000), in print.
19) J.-O. ANDERSSON amd J. AGREN, *J.Appl.Phys*. 72, (1992), p.1350.
20) J.O. ANDERSSON, L. HOEGLUND, B. JOENSSON and J. AGREN, *Fundamentals and Applications of Ternary Diffusion*, G.R. PURDY (Ed.), Pergamon Press, NY (1990), p.153.
21) R.D. DOHERTY, *Physical Metallurgy*, R.W. CAHN, P. HAASEN (Eds.), Elsevier, Amsterdam (1983), p. 942.
22) A.K. SINHA, *Ferrous Physical Metallurgy*, Butterworth, Stoneham (1989=, p. 121.
23) S. PARK and J.J. JONAS, *Met.Trans.* 23A, (1992), p.1641.
24) A.H. COTTRELL, *Report on Strength of Solids*, The Physical Society, London (1948).
25) M. MILITZER, W. SUN and J.J. JONAS, *Microstructure and Properties of Microalloyed and other Modern High Strength Low Alloy Steels*, M. DeARDO (Ed.), Pittsburgh (1991).
26) R. WAGNER and R.KAMPMANN, *Materials Science and Technology Vol.5*, P. HAASEN (Ed.), VCH, Weinheim (1990), p.213.
27) R. SANDSTROEM and R. LAGNEBORG, *Acta Met.* 23, (1975), p.387.
28) J.P. SAH, G.J. RICHARDSON and C.M. SELLARS, *Metall.Sci*. 8, (1974), p.325.
29) W. ROBERTS and B. AHLBLOM, *Acta Met*. 26, (1978), p.801.
30) C. ZENER, *T.M.S.-A.I.M.E.* 175, (1949), p.175.
31) J.W. CAHN, *Acta Met*. 10, (1962), p.789.